Improvement of a Computer Tool for the Different Modes Optimization of Heat Transfer in a Monobloc House

Oudrane Abdellatif[1*], Aour Benaoumeur[1], Hmouda Messaoud[2], Damba Nadir[1] and Benyoub Mohammed[1]

[1]Laboratory of Applied Biomechanics And Biomaterials (LABAB), BP 1523 El Mnaour, National Polytechnic, School of Oran-Maurice Audin (ENPO-MA), Oran 31000, Algeria

[2]Laboratory of Sustainable Development and Informatics (LDDI), Faculty of Science and Technology, Ahmed Draia University of Adrar, 01000, Algeria

***Corresponding author's email:** abdllatif.habadat@gmail.com

Received: 29 August 2022, Revised: 14 September 2022, Accepted: 22 December 2022

Abstract

The main role of this work is to develop a computer calculation program to estimate the different modes of heat transfer for a habitable envelope equipped with a heating plate in order to optimize thermal comfort. This optimization is based on the use of real climate data from the region under consideration. To achieve this goal, we have developed five fundamental codes in FORTRAN language. The first code consists in modeling the flow of the heat transfer fluid in the heating slab pipe. The second is designed to model the heat transfer by conduction within the concrete slab. The third is developed for the modeling of thermal exchanges in a habitable envelope assimilated to a parallelepiped cavity based on the nodal method. The fourth code is reserved for the modeling of solar radiation by evaluating the wage flux density on different positions of the walls. The fifth and last code is dedicated to the evaluation of the perfect thermal coupling between the concrete slab and the heat transfer fluid pipes. The validation of the models implemented in the calculation codes was made on the basis of data measured recently for a clear sky of solar radiation at the radiometric station of the renewable energies research unit in the Saharan environment URER'MS of ADRAR. The results obtained showed a very good agreement between the calculated values using the computational codes developed and those measured by the radiometric station of the URER'MS during the typical day.

Keywords:

Heat Transfer; Saharan Environment; Heating Slab; Renewable Energies; Thermal Comfort; Solar Energy; Radiometric Station

1. Introduction

Solar energy is the source of the cycle of water, wind and photosynthesis carried out by the plant kingdom, on which the animal kingdom depends via the food chains. The sun is at the origin of most of the energies on Earth, except for nuclear energy and deep geothermal energy. The times of sunrise and sunset, as well as the sun path in the sky during a day, allow us to assess quantities, such as the maximum duration of insolation, the solar flux and the ambient temperature [1]. Solar energy is used in different ways, either in photovoltaic systems for the electricity production or in thermal systems (solar water heaters) for the hot water production, a field in which it is experiencing considerable development, particularly in the habitat sector [2].

Zarai et al. [3] presented the design of a sizing and planning code for the production of a solar thermal installation by making an estimate of the evolution of the global solar flux and ambient temperature during a daytime. All results are visualized through graphical interface designed using Matlab software. The development of buildings contributes mainly to the challenges of the energy transition to better reduce its consumption, ensure better comfort, meet environmental and regulatory requirements, while minimizing the total price. Abbass et al. [4] proposed a numerical tool design from

the sketch phase to the more advanced design phase. This numerical tool is based on solutions offering a global vision of the building and allowing to make optimal choices using the internet, to cover the aspects of global modeling and decision support.

Dinh et al. [5] presented an optimal sizing methodology integrating the management strategy of a complex energy system (heating, air conditioning, PV and electrochemical storage) for a building connected to the network. They approved that the thermal comfort is determined through a reduced order dynamic thermal envelope model, and life-cycle cost is considered as optimization criteria while load coverage is considered as one of the constraints.

Oudrane et al. [6] have established an adequate methodology to properly dimension and optimize the geometric and thermal parameters of the solar system (PSD). The latter has been implemented in a computational code to automate the optimization procedure.

In this context, the objective of this paper is to develop computer tools to model and optimize thermal comfort in a habitat. It is important to note that such tools can be used by architects and design offices for the prediction of the habitat energy behavior and its adequacy with current standards. To achieve this objective, we started with a presentation of the mathematical formulation. A conclusion on the obtained results is presented at the end of this work.

2. General description of the computer codes

The developed computer codes are programs established for performing thermodynamic simulations of a habitable envelope. We started in the first part by implementing numerical models for modelling the heat transfer of the hot water flow in the heating slab pipe. For this, we have based on the Navier-Stokes and the heat equations that govern this flow. These equations have been discretized by an implicit finite difference method. The resulting system of algebraic equations was solved using Gauss and Thomas algorithms [7-8].

Then, in a second phase, we implemented the conduction equation in the concrete slab using the same methodology as for the flow. The heat transfers that take place in a habitat model assimilated to a parallelepiped cavity have been modelled using the thermal balances established at each wall of the habitat and taking into account heat exchanges by convection, conduction and radiation [9].

The calculation in this phase consists in reducing a model to finite differences by modal analysis. Non-linear quantities are introduced in the simulation phase. This tool has been improved and completed by the generation of hourly weather files of different components of the daily solar flux, files of incident solar flux for each face of the habitable envelope, as well as their external and internal temperatures in each hour of the typical day. Noting that this tool is flexible and accessible to solar thermal researchers. In order to spread out this description, we have subdivided this computer tool into five fundamental computational codes which have been named as follows:

- **CFD:** Code for the Fluid Dynamics in the slab pipe.
- **CHC:** Code of the Heat Conduction in the slab.
- **CTC:** Code for the fluid-structure Thermal Coupling.
- **CTE:** Code of the Thermal Exchange modeling in the habitat.
- **CSR:** Code of the Solar Radiation evaluation.

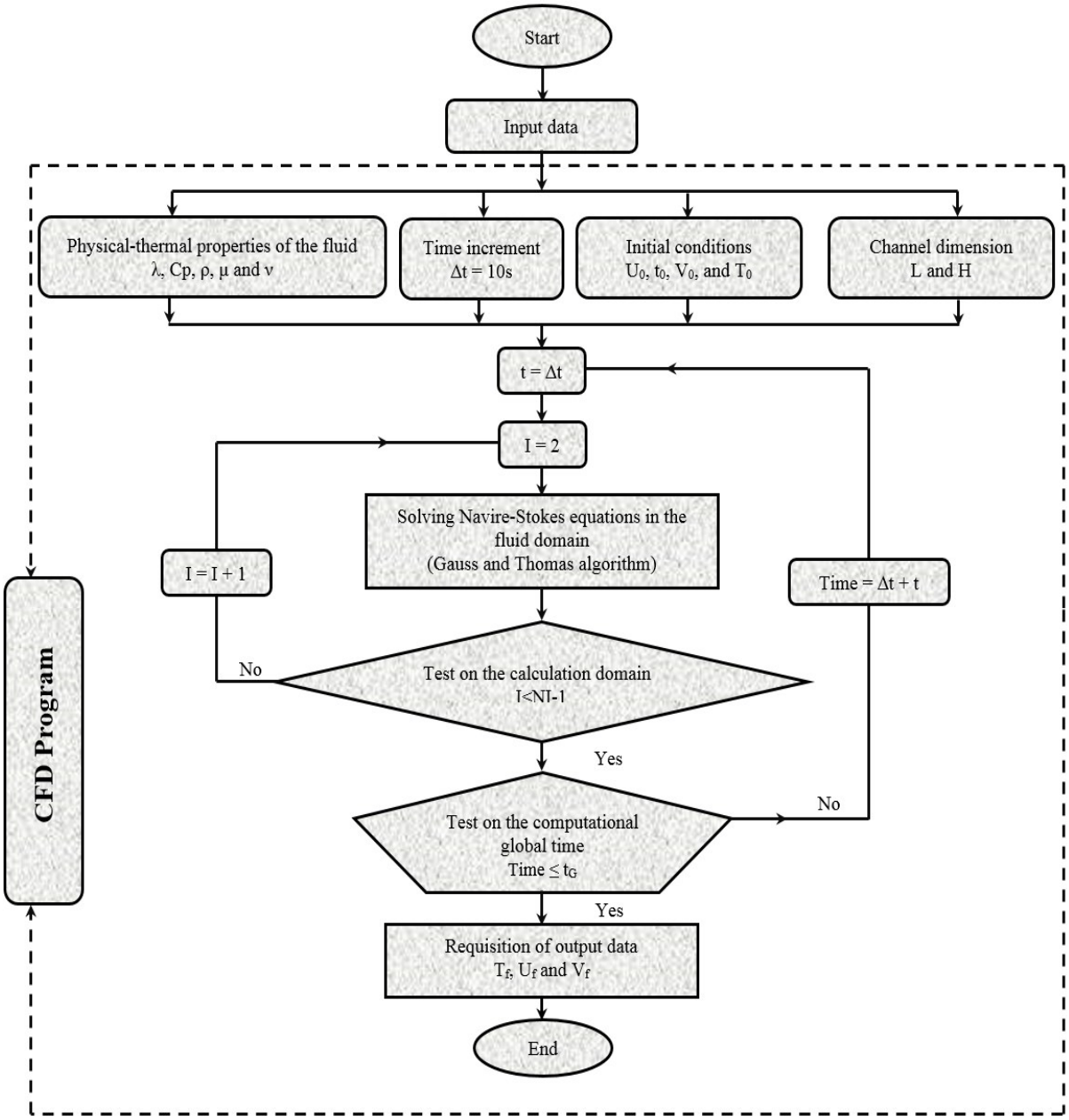

Fig. 1 Flowchart of fluid flow modelling in the pipe using CFD code.

2.1. Description of CFD code

The CFD code is a program developed for solving the differential equations that govern the mass transport, momentum, laminar variables and energy. In this study, we are interested to the modelling of the coolant flow, as well as the heat and mass transfer processes in the concrete slab pipe. The calculation steps are detailed by the flowchart is shown in Fig. 1.

2.1.1. Input Data for CFD code

In the two tables below, we show the different types of operating data in the CFD code.

Table 1 CFD input data.

CFD-Input data		
Normal index	**Designation**	**Code index**
U_0 *and* V_0	Fluid velocity in ($m.s^{-1}$)	UU_0 *and* VV_0
t_0	Initial time in (s)	*TTEMPS*
Re	Dimensionless Reynolds number.	*RRE*
T_{amb}	Ambient temperature in (K)	*TTAMB*
d	Pipe diameter in (m)	*HHAUT*
l	Pipe length in (m)	*LLONG*
Δx *and* Δy	Space increment for both axes (abscissa and ordinate)	*DDX and DDY*
Δt	The time increment step in (s)	*DDELTAT*
t	Global calculation time in (s)	*GGTEMPS*
	Physico-thermal properties of the fluid	
λ	Thermal conductivity of the fluid in ($W.m^{-1}.K^{-1}$)	*LLANDA*
Cp	Heat capacity of the fluid in ($J.kg.K^{-1}$)	*CCP*
ρ	Mass density of the fluid in ($kg.m^{-3}$).	*RROH*
μ	Dynamic viscosity of the fluid in ($kg.m^{-1}.s^{-1}$).	*MMU*
υ	Kinematic viscosity of the fluid in ($m^2.s^{-1}$).	*NNU*
Pr	Prandtl dimensionless number of the fluid	*PPR*

Table 2 CFD code output data.

CFD-Output data		
Normal index	**Designation**	**Code index**
V_f	Transverse velocity of the fluid in ($m.s^{-1}$)	*VV*
U_f	Longitudinal velocity of the fluid in ($m.s^{-1}$)	*UU*
T_f	Fluid temperature in (K)	*TT*

2.1.2. Main program of CFD code

```
PROGRAM FLUID_FLOW
  IMPLICIT NONE
  DOUBLE PRECISION LONG,HAUT,DXA,DYA,U1(200,200),V1(200,200)
          CALL DOMAINE(LONG,HAUT)
  CALL PORPREAU(MU,LANDA,CP,RHO,NU)
  CALL DONN(RE,PR,MU,LANDA,CP,RHO,NU,U0,HAUT,TE,TP1,TP2,TEMPSG)
   I=2
   CALL LIMIT(NJ,I,U2,V2,T2,TE,TP1,TP2)
   CALL DEBIT(U2,DEB,NJ,DYA)
   CALL COEFGAUSS(A,B,C,D,MG,J,NJ,DEB,Y,DELTAT,U1,V1,U2,DXA,DYA,RE)
   CALL GAUSS(NJ-1,MG,Y,XG)
  DO 12 J=1,NJ-2
   U2(I,J+1)=XG(J)
  P=-1.D0
   GRADP(I)=XG(NJ-1)
  P(I)=P(I-1)+(GRADP(I-1)*DXA)
```

```
      CALL MOYENNE(I,NJ,U2,MOYPHI)
      MOYUAP=MOYPHI
      ERRU=ABS((MOYUAP-MOYUAV)/MOYUAP)
  300 CALL MOYENNE(I,NJ,T2,MOYPHI)
      MOYTAV=MOYPHI
      DO J=1,NJ
      TAV(J)=T2(I,J)
      ENDDO
      CALL LIMIT(NJ,I,U2,V2,T2,TE,TP1,TP2)
      CALL THOMAS(2,NJ-1,A,B,C,D,X)
      CALL LIMIT(NJ,I,U2,V2,T2,TE,TP1,TP2)
      END
```

2.2. Description of CHC code

The CHC code is dedicated to the thermal behavior simulation of the concrete slab under the thermal diffusion action due to the fluid flows in the pipes embedded in the slab. To achieve this objective, a numerical model governing heat conduction is implemented in a computer program in order to calculate and determine the maximum real temperature gradient in the slab based on finite difference calculations that are used to determine the equivalent linear gradient in the slab which will be used for its sizing. The detailed flowchart of this calculation code is shown by Fig. 2.

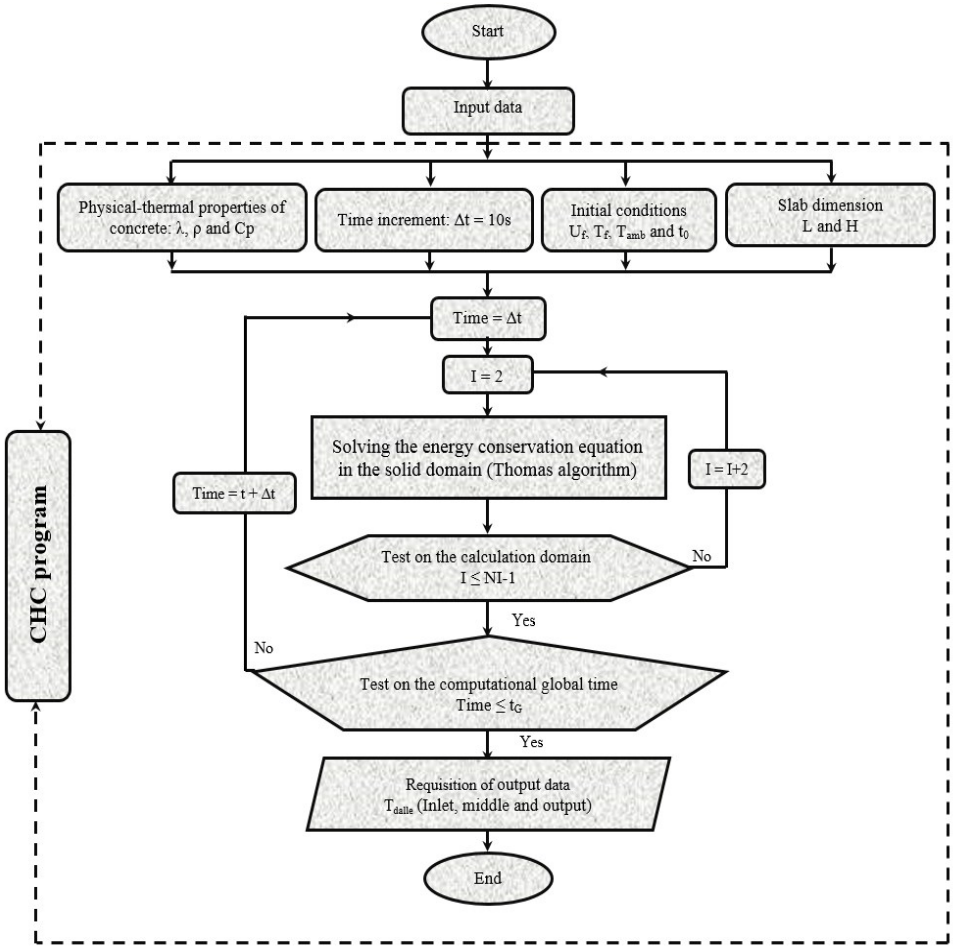

Fig. 2 Flowchart of heat conduction modelling in the solid using CHC code.

2.2.1. Input data for CHC code

In the two tables below, we indicate the different types of the CHC code operating data.

Table 3 CHC Input Data.

CHC-Inputs data		
Normal index	**Designation**	**Code index**
L	Slab length in (m)	*LLONG*
ep	Slab thickness in (m)	*HHAUT*
Δx *and* Δy	Space step for both axes (abscissa and ordinate)	*DDX and DDY*
Δt	The time increment step in (s)	*DDELTAT*
t	Global calculation time in (s)	*GGTEMPS*
Physico-thermal properties of Concrete		
λ_b	Thermal conductivity of concrete in ($W.m^{-1}.K^{-1}$)	*LLANDAB*
ρ_b	Mass density of concrete in ($kg.m^{-3}$)	*RROHB*
Cp_b	Heat capacity of the fluid in ($J.kg.K^{-1}$)	*CCPB*
T_{amb}	Ambient temperature in (K)	*TTAMB*

Table 4 CHC Ouput Data.

CHC-Ouput data		
Normal index	**Designation**	**Code index**
$T_{entré\ dalle}$	Temperature at the slab entrance in (K)	$TT_{entré\ dalle}$
$T_{milieu\ dalle}$	Temperature in the slab middle in (K)	$TT_{entré\ dalle}$
$T_{sortie\ dalle}$	Temperature at the slab exit in (K)	$TT_{entré\ dalle}$

2.2.2. Main program of CHC code

```
      PROGRAM DIFFUSION_DALLE
      IMPLICIT NONE
      DOUBLE PRECISION
      LONG,HAUT,DXA,DYA,DELTAT,U0,LANDAB,CPB,ROHB,NU,MU
      DOUBLE PRECISION ROH,RE,TBP1,TB1(200,200),TB2(200,200),T0
      DOUBLE PRECISION EPS
      INTEGER I,K,NI,NK,Z,N,L,Y,H
      EPS=1.D-3
      CALL DOMAINE(LONG,HAUT)
      CALL PROPRBETON(LANDAB,CPB,ROHB,NU,MU,ROH)
      CALL DONNEES(RE,U0,TBP1,HAUT,TEMPSG,PRG,NU,CPB,T0,ROHB,LANDAB)
70    CALL MAILLAGE(NI,NK,HAUT,LONG,DXA,DYA,DELTAT,U0)
      CALL INIT(NI,NK,TB1,TB2)
      TEMPS=DELTAT
80          CONTINUE
      CALL MOYTDOM(NI,NK,TB2,MOYTBDAV)
      I=2
        TB2(I,K)=X(K)
50        CONTINUE
      CALL LIMIT(I,NK,TB2,TBP1,T0)
        ENDDO
      END
```

2.3. Description of CTC code

The CTC code is a numerical tool for simulating fluid-structure thermal coupling in order to describe the state of matter throughout the structure based on the explicit finite difference method. The coupling is associated with Gauss and Thomas algorithms for the iterative resolution of the algebraic system [10-11]. The purpose of the CTC computer program is to characterize the thermal exchange in variable regime between a hot fluid flow in forced convection and a concrete slab, in which the upper face is subjected to ambient temperature. Figure 3 shows the detailed flowchart for this computer code (CTC).

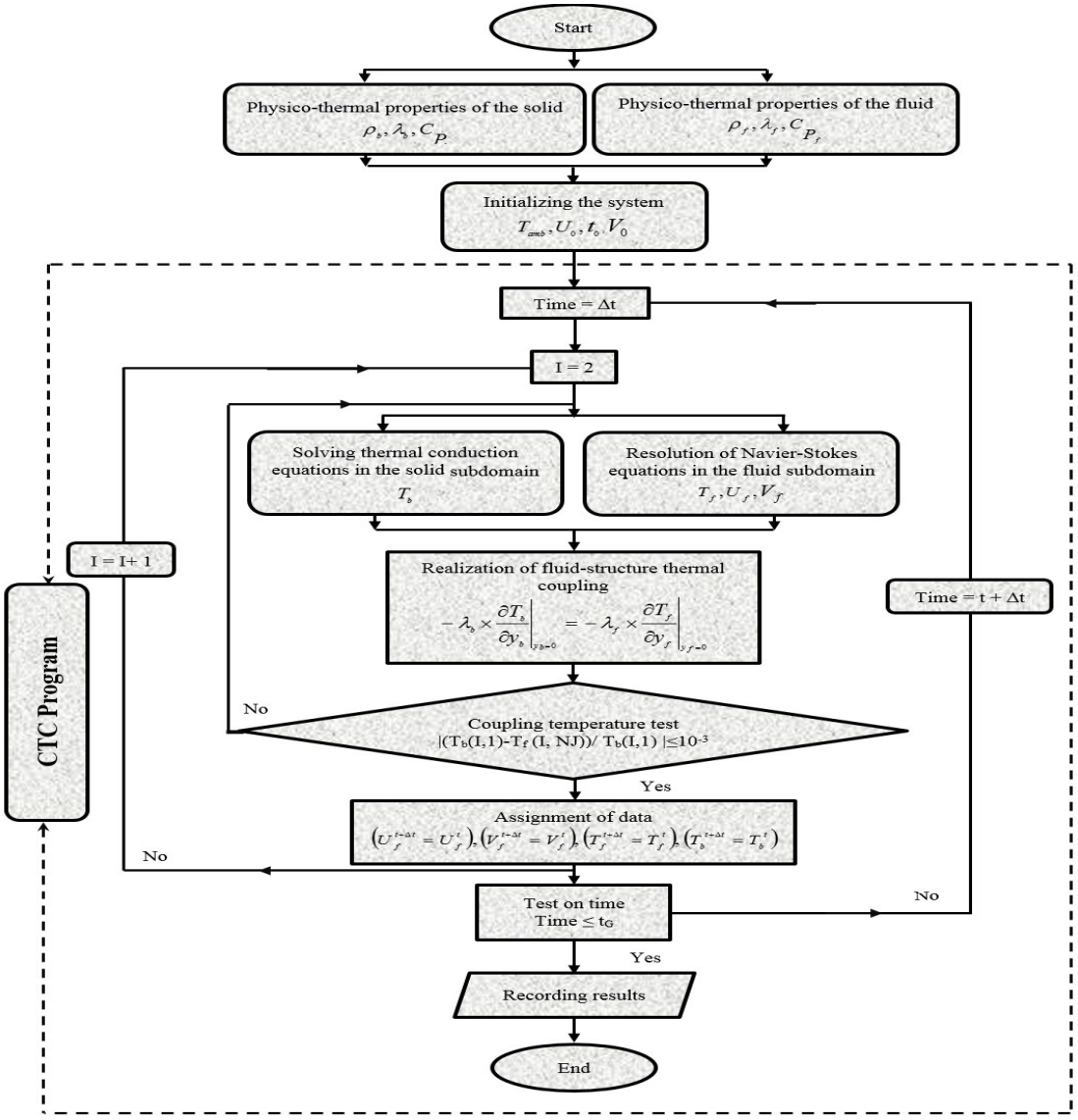

Fig. 3 Flowchart of the perfect thermal fluid-structure coupling using CTC code.

2.3.1. CTC code input data

The input and output data tables of this Fluid-Structure thermal coupling computer tool are the set of input and output data of CFD and CHC codes mentioned before in the tables (1, 2, 3 and 4).

2.3.2 Main program of CTC code

```
      PROGRAM COUPLAGE_TUBE_SLAB_HABITAT
      IMPLICIT NONE
      DOUBLE PRECISION HAUTF,HAUTB,LONG,DXA,DYFA,DYBA,U2(200,200)
      DOUBLE PRECISION TE,U0,TEMPSG,PRF,NUF,CPF,LANDAF
      CALL MAILLAGESYSTE(NI,NJ,NK,NJK,LONG,HAUTF,DXA,DYFA,DYBA,DYA)
      CALL     PROPRMATERIE(MUF,LANDAF,CPF,ROHF,NUF,LANDAB,ROHB,CPB,LANDA
       ,RAPROCP)
      CALL DONNEENTRE(HAUTF,CPF,CPB,NUF,MUF,LANDAF,LANDAB,ROHB,PRF,
         I=2
111   CONTINUE
      CALL MOYDOMFLUID(NI,NJ,T2,MOYPHI)
      MOYDTAV=MOYPHI
112   CALL MOYENTRNCHFLU(I,NJ,U2,MOYPHI)
      MOYUAV=MOYPHI
      P=-1.D0
      CALL MOYENTRNCHFLU(I,NJ,U2,MOYPHI)
      CALL MOYENTRNCHDAL(I,K,NK,TB2,MOYPHI)
      MOYTBAV=MOYPHI
117      CONTINUE
         CALL LIMITDALLE(I,NJ,NK,LANDA,DYA,T2,TB2,T0,TE)
         I=I+1
      CALL MOYDOMFLUID(NI,NJ,T2,MOYPHI)
                        DO K=1,NK-1
            DO I=2,NI-1
              TEMP(I,NJ+K)=TB2(I,K+1)
            ENDDO
             ENDDO
            IMID=0.5*(NI+1)
      END
```

2.4. Description of CTE code

The CTE calculation code is dedicated to the modeling of the different transfer modes in the studied habitable envelope and the surrounding atmosphere. In this code, we have implemented a numerical model to describe the exchanges of energy and mass that take place between both media (the atmosphere and the habitat) and which therefore imply their interdependence [12].

However, the microclimate affects the internal thermal conditions of the habitat, and consequently its energy behavior in different ways. For this reason, we have considered, firstly, the direct and diffuse solar radiations, which are altered by the elements of the habitat and by the building materials and, secondly, the temperature and velocity of the outside air, which influence the conductive and convective exchanges between the habitat and its environment. The effects of conduction in the walls on the interior environment of the habitable envelope and its thermal insulation have also been considered [12-13]. The numerical processing in this computer program was done using the Gauss algorithm [13]. All parts of the habitat are subject to heat transfers, which are heat exchanges between the hot and cold environments (usually from the outside to the inside). The flowchart, in Figure 4, shows the main stages of the heat exchange occurring within the habitable envelope.

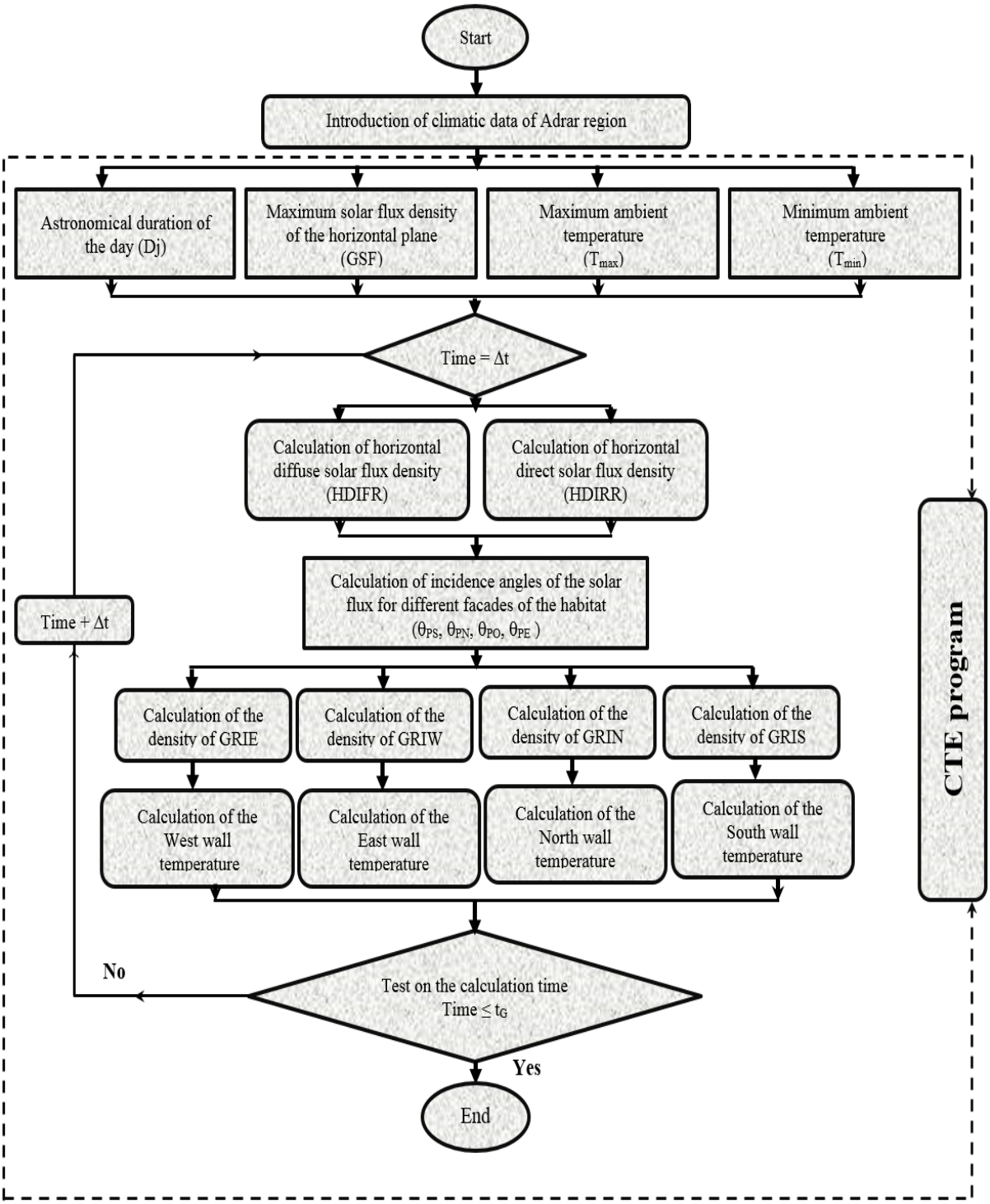

Fig.4 Flowchart of heat exchange modelling in the habitat using CTE code.

2.4.1. CTE code input data

In the two tables below, we present the different types of data used by CTE code.

Table 5 CTE code input data.

CTE-Input data		
Choice of day Type		
Normal index	**Designation**	**Code index**
T_{amb}	Ambient temperature in (K)	*TTAMB*
t	Global calculation time in (s)	*GGTEMPS*
RSH	Global horizontal solar flux in ($w.m^{-2}$)	*RRGHV*
RSS	Incident solar flux on the south wall in ($w.m^{-2}$)	*RRGIS*
RSN	Incident solar flux on the north wall in ($w.m^{-2}$)	*RRGIN*
RSO	Incident solar flux on the west wall in ($w.m^{-2}$)	*RRGIO*
RSE	Incident solar flux on the east wall in ($w.m^{-2}$)	*RRGIE*
a	Width of the habitable envelope in (m)	*LLARGH*
b	The habitable envelope height in (m)	*HHAUTH*
c	The habitable envelope length in (m)	*LLONGH*
e	Wall thickness of the habitable envelope in (m)	*EEP*
S_p	Wall surfaces of the habitable envelope in (m^2)	*SSP*
NOC	Number of occupants in the habitable envelope	*NOC*
GCS	Sensitive heat sheath of the individual in (w)	*GCS*
GCL	Sheath of latent heat of the individual in (w)	*GCL*
η_{50}	Hourly air renewal rate in (h^{-1})	*WW*
e_i	Local wind exposure coefficient	*EE*
ε_i	Corrective coefficient for habitat height	*NNB*
S_{inf}	Air infiltration area in the habitat in (m^2)	*SSPet*
V_{MV}	Average wind speed in ($m.s^{-1}$)	*VVMV*
T_{sol}	Soil temperature in (K)	*TTSOL*
$T_{Plancher}$	Floor slab temperature in (K)	*TTB*
λ_P	Thermal conductivity of walls in ($W.m^{-1}.K^{-1}$)	*LLANDAP*
Cp_P	Heat capacity of the walls in ($J.kg.K^{-1}$)	*CCPP*
λ_{air}	Thermal conductivity of air in ($W.m^{-1}.K^{-1}$)	*LLANDAA*
Cp_{air}	Heat capacity of air in ($J.kg.K^{-1}$)	*CCPA*
ρ_{air}	Mass density of air in ($kg.m^{-3}$)	*RROHA*
μ_{air}	Dynamic viscosity of air in ($kg.m^{-1}.s^{-1}$)	*MMUA*
ν_{air}	Kinematic viscosity of air in ($m^2.s^{-1}$)	*NNUA*
Pr_{air}	Dimensionless Prandtl number of air	*PPRA*
ε_P	Coefficient of wall emissivity	*EEMSP*
α_P	Coefficient of the wall absorption	*AALPHAP*

Table 6 CTE code output data.

CTE-Output data		
Normal index	**Designation**	**Code index**
TPSE	Temperature of the external facade of the south wall in (K)	*TTPSE*
TPNE	Temperature of the external facade of the north wall in (K)	*TTPNE*
TPOE	Temperature of the outer facade of the west wall in (K)	*TTPOE*
TPEE	Temperature of the external facade of the wall in (K)	*TTPEE*
TPPE	Temperature of the external facade of the ceiling wall in (K)	*TTPPE*
TPSI	Temperature of the internal facade of the south wall in (K)	*TTPSI*
TPNI	Temperature of the internal facade of the north wall in (K)	*TTPNI*
TPOI	Temperature of the internal facade of the west wall in (K)	*TTPOI*
TPEI	Temperature of the internal facade of the wall in (K)	*TTPEI*
TFPI	Temperature of the internal facade of the back-ceiling wall in (K).	*TTFPI*
TAI	Temperature of the internal space of the habitat in (K)	*TTAI*

2.4.2. Main program CTE

```
      PROGRAM HABITAT_RADIATION
      IMPLICIT NONE
      DOUBLE PRECISION F3,F4,F5,F6,F7,F8,F9,F10,R1,R2,T2POS_AV,ERR_TPSI
      DOUBLE PRECISION R10,R11,R12,R13,R14,R15,R16,R17,ERR_TPEE,ERR_TPEI
 DO          100     HEUR=1,24
             READ(1100,*)TA1V(HEUR)
100               CONTINUE
             CLOSE(1100)
 DO     200    HEUR=1,24
            READ(2200,*)RGHV(HEUR)
200          CONTINUE
             CLOSE(2200)
          CALL
DIMENSHABIT(LONGPN,HAUTH,EPS,LONGPS,LONGPO,LONGPE,LONGPFP,LARGPFP,LO
NGPIP,LARGPIP)
CALL PROPRIETESMA(LANDAA,CPA,ROHA,MUA,NUA,G,LANDAB,CPB,ROHB,
EMSB,ALPHAB)
CALL SURFACE_MASSE(LONGPN,HAUTH,ROHB,EPS,LONGPS,ROHA,LONGPIP,
LARGPIP,LONGPFP,LONGPO)
I=1
TEMPS=DELTAT
CALLINITIA(T1PSE,T1PNI,T1POE,T1POI,T1PEE,T1PEI,T1PFPE,T1PFPI,T2PSI,T2PNI,T2POE,
T2POI,T2PEE,T2A2,TA1V,TA1,TSOL)
90   CONTINUE
               I=I+1
          IF((ERR_TPSE.GT.EPSIL).OR.(ERR_TPSI.GT.EPSIL).OR.(ERR_TPNE.GT.
         &  EPSIL).OR.(ERR_TPNI.GT.EPSIL).OR.(ERR_TPOE.GT.EPSIL).OR.
                GOTO 90
         END IF
             IF(Mod(TEMPS,3600).EQ.0) THEN
             END IF
             IF(TEMPS.LT.86400)THEN
             TEMPS=TEMPS+DELTAT
          GOTO 90
         END IF
         END
```

2.5. Description of CSR code

The purpose of the CSR code is to calculate the solar flux values in a typical day. The calculation through this code is based on the assignment of the values of the meteorological variables acquired by the nearest radiometric station [14]. It should be noted that the extraction of the different components of solar radiation from meteorological data depends closely on the exact knowledge of geographical coordinates (latitude, longitude, altitude, etc.) of the position corresponding to the given pixel and the values of the meteorological variables.

The calculation of the solar flux using the CSR code facilitates the optimization of different thermal exchanges within a habitat in order to achieve a pleasant and conventional comfort. The detailed flowchart of the CSR calculation code is given by Fig. 5.

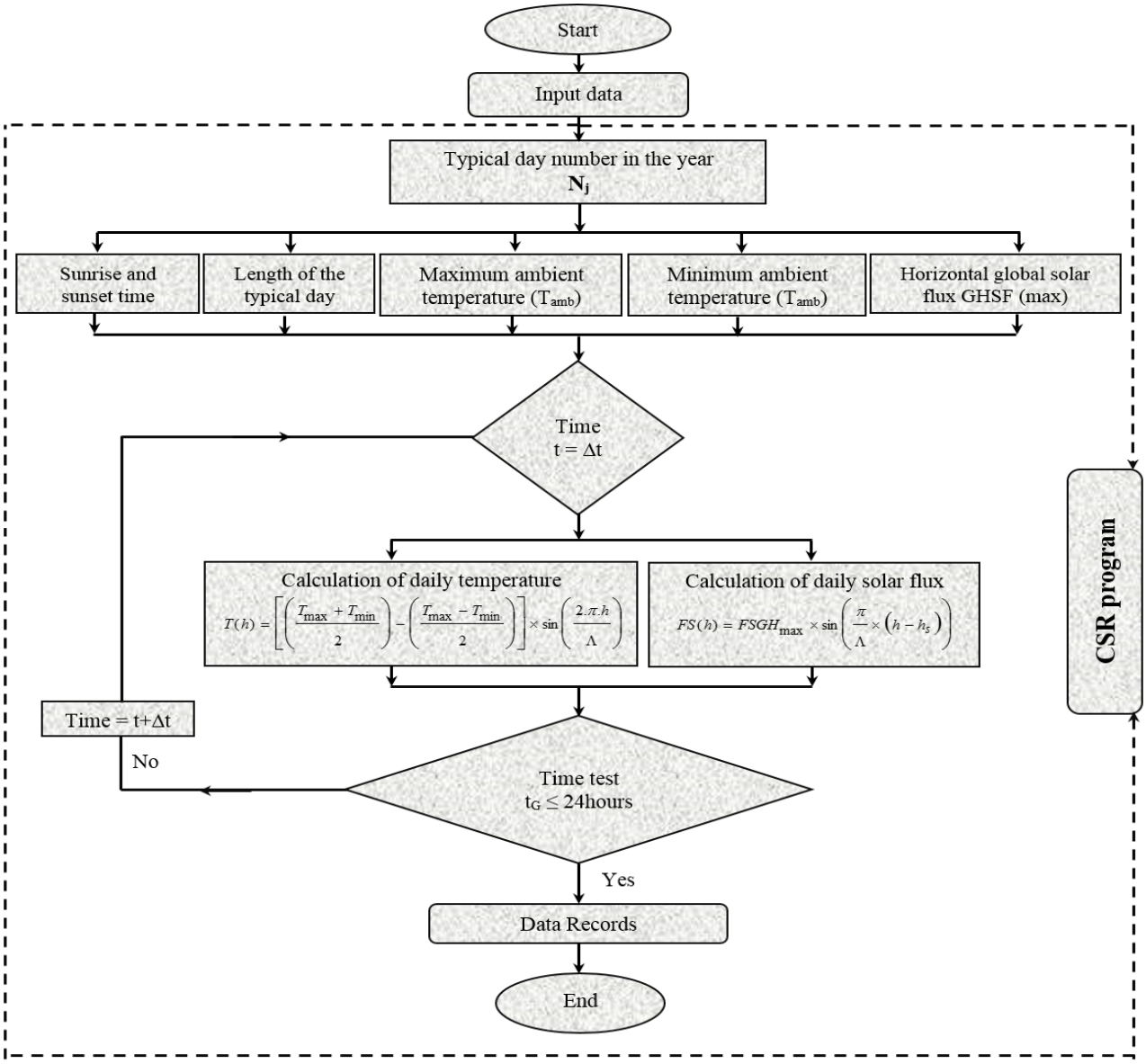

Fig.5. Flowchart of solar radiation modelling using CSR code.

2.5.1. CRS Code Input Data

In the two tables below, we present the different types of operating data in the CRS code.

Table 7 CRS Input Data.

CRS-Inputs data		
Choice of typical day		
Normal index	**Designation**	**Code index**
D_j	Duration of the typical day in (h)	*DDJ*
FSG_{Max}	Maximum horizontal global solar flux in (w.m^{-2})	*FFSGM*
$Tamb_{Max}$	Maximum ambient temperature in (k)	*TTAMAX*
$Tamb_{Min}$	Minimum ambient temperature in (k)	*TTAMIN*
Nj	Number of the day in the year from January 1st	*NNj*
ALBE	Soil albedo coefficient	*AALBE*
λ	Longitude of location in (°)	*LLONGI*
φ	Latitude of location in (°)	*LLATD*
t	Global calculation time in (s)	*GGTEMPS*

Table 8 CRS Output Data.

CRS-Output Data		
Normal index	**Designation**	**Code index**
FSG	Global daily solar flux in (w.m^{-2})	*RRHGV*
T_{amb}	Daily ambient temperature in (k)	*TTAV*
ω	Hour angle of the sun in (°)	*OOMEGA*
a_z	Sun azimuth by degrees (°)	*ZZM*
h	Angular height of the sun in (°)	*hh*
RDIRH	Horizontal direct solar flux in (w.m^{-2})	*RRDIRH*
RDIFH	Horizontal diffuse solar flux in (w.m^{-2})	*RRDIFH*
RGIS	Solar flux incident on the south wall in (w.m^{-2})	*RRGIS*
RGIN	Solar flux incident on the north wall y (w.m^{-2})	*RRGIN*
RGIE	Solar flux incident on the east wall in (w.m^{-2})	*RRGIE*
RGIO	Solar flux incident on the west wall in (w.m^{-2})	*RRGIO*

2.5.2.Main program CRS

```
PROGRAM METEO
   IMPLICIT NONE
   DOUBLE PRECISION TTE,TAMAX,TAMIN,FID,TTO,Y1(35),Y2(35)
   INTEGER HHEUR
            TTHM=12.D0-DDJ/2.D0
   FID=1.D0
   DO 20 HHEUR=1,24
   IF ((HHEUR.GE.KOL).and. (HHEUR.LE.SOL)) THEN
   FFLUX=AA*SIN(OOM*(HHEUR-TTHM))
   ELSE
   FFLUX=0.D0
   ENDIF
   IF ((HHEUR.GE.KOL+1).and.(HHEUR.LE.SOL+1)) THEN
   TTE=((TAMAX+TAMIN)/2.D0)-((TAMAX-TAMIN)/2.D0)*SIN(((1.D0*PI*HHEUR)/TTO)-
FID)+273.15D0
   ELSE
   TTE=273.15D0+TAMIN
   ENDIF
   END
```

3. Code testing

3.1. Physical model studied

In what follows, we present the main characteristics of the studied habitable envelope. This latter has a concrete structure of height 'b', width 'a' and length 'c' with opaque walls of thickness 'e' along the facades (Figure 6-a). Internal heating is provided by the floor slab, which consists of three layers comprising a serpentine tube (Figure 6-b). The first layer is a thermal insulating expanded polystyrene sheet. The height of the layer for insulation is 5 cm. Above it, we have a concrete screed of height ‘f’, length ‘c’ and width ‘a’. In the latter are arranged the cross linked polyethylene tubes which are very often used for the realization of heating floors [15-16]. Indeed, these semi-rigid pipes are flexible, which are arranged in U-shape with a diameter of 20mm and a spacing of 10cm [16]. A concrete covering layer is superimposed on the heating grid. In summer, thermal comfort is provided by opening windows, using blinds and natural ventilation [17].

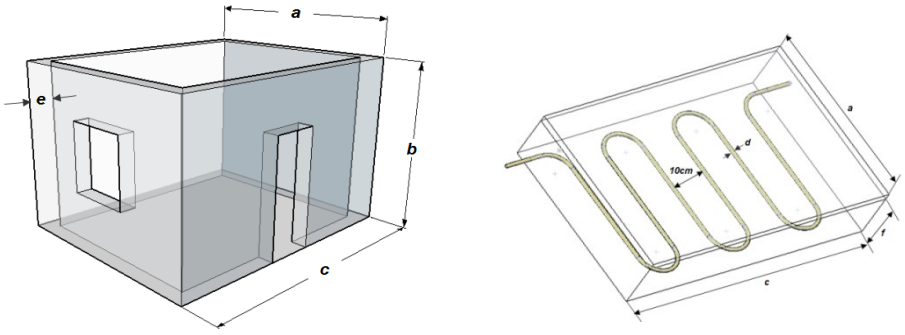

(a) The considered habitable envelope. (b) The floor slab of the habitat.

Fig.6. Description of the different compartments of the studied physical model.

3.2. Simplifying assumptions

In this study, we have assumed the following assumptions:

- Transfers are unidirectional;
- The thermal inertia of the air is negligible;
- The air is perfectly transparent to solar radiation;
- The habitat is not a seat of any mass transfer;
- The materials are assimilated to gray bodies;
- The thermophysical properties of materials are constant;
- The celestial vault behaves like a black body;
- The diffuse atmospheric radiation is isotropic;
- The air renewal rate is only considered within the habitat enclosure.

3.3. Physico-thermal description of the studied habitable envelope

The habitable envelope simulated in this case study is a mono-zone of 20m^2 in area and 3m in height built on flat earth. It is made of molded earth bricks, then dried in the sun [18-19]. The thermo-physical characteristics are summarized in table 9:

Table 9 Thermo-physical characteristics of the materials constituting the habitable envelope studied [18-19].

Walls	Material	$\lambda\,(W.m^{-1}.k^{-1})$	$\rho\,(kg.m^{-3})$	$Cp\,(kJ.kg^{-1}.k^{-1})$	α	ε	$e\,(cm)$
South wall	Molded earth	1,10	1900	1500	0,80	0,91	20
North wall							
East wall							
West wall							
High floor	Molded earth						
	Palm waste	0,09	350	1000	0,60	0,90	20
Low floor	Full earth	1,10	1900	1500	0,80	0,91	20

3.4. Choice of the typical day

It is possible to determine the monthly typical day (defined by a characteristic declination) and which has a daily irradiation equal to the monthly average. The recommended day for each month with the corresponding day number of the year are given in Table 2. As a result, the monthly averages can be deduced from the daily sums of extra-terrestrial solar radiation, as follows [20]:

$$\overline{H_0} = H_0\big|_{\delta=\delta c} \tag{1}$$

Knowing that, the daily amount of extra-terrestrial solar radiation is expressed by:

$$H_0 = \frac{24}{\pi} I_0 \left(\frac{\pi}{180} .\omega_s .\sin\delta .\sin\varphi + \cos\delta \cos\varphi .\sin\omega_s \right) \tag{2}$$

3.5. Interpretation of climatic data of the typical day

In fact, our choice in this case study is based on the notion of the typical day. Based on the climatic data measured by the radiometric station (Figure 7) of the Research Unit for Renewable Energies in the Saharan Environment (URER'MS) of the TOUAT region of ADRAR, we chose July 17th, 2016 as the typical day.

Fig. 7 Photograph of the meteorological station installed at URERMS in Adrar.

3.6. Results and discussion

3.6.1. Validation

Figure 8 shows a comparison between the calculated and measured values of the global horizontal solar flux and the direct horizontal flux as a function of the local time of the typical day considered. It is found that there is an acceptable agreement between the results obtained by the developed model and those measured by the URER'MS radiometric station of ADRAR, with relative errors equal to 1.44% for the global flux and 1.25% for the direct horizontal flux.

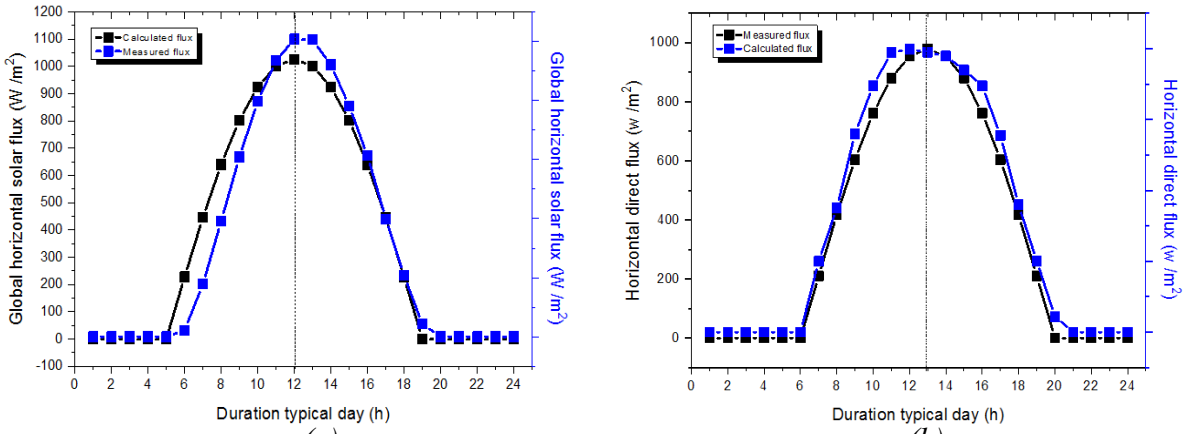

Fig. 8 Comparison between the calculated and measured values of (a) the horizontal global solar flux and (b) the horizontal direct flux in a typical day as a function of the local time.

3.7. Conclusion

The work carried out in this paper has two main objectives. The first is to develop a computer tool for numerical simulation of thermal exchanges in buildings. The second is devoted to the estimation of the amount of solar flux incident on the different facades of a habitat based on real measured climatic data in order to optimise thermal comfort. The case study that was presented using the developed calculation programs showed that it is possible to highlight the instantaneous evolutions of the different components of the incident solar flux on a surface with any orientation and inclination. From the results presented above, the following conclusions can be drawn:

- The comparison of the values estimated by the developed models and the measured values provided by (URER'MS) of Adrar Radiometric Station proves to be acceptable on the whole.

Finally, we can say that these computational codes can then be coupled to a professional and user-friendly interface so that it can be easily used by specialists in this field and work on this way is under investigation.

Nomenclature

a	Width of the wall	m
A	Considered exchange area	m^2
b	Height of the wall	m
c	Length of the wall.	m
Cp	Specific heat of the fluid	$kJ.Kg^{-1}.K^{-1}$
d	Tube diameter	m
e	Wall thickness	m
Gr	Dimensionless Grashof number	-
$\overline{H_0}$	Monthly average of daily amounts of solar radiation	$W.m^{-2}$
H_0	Daily sum of extra-terrestrial solar radiation	$W.m^{-2}$
h	Height of the sun	$(°)$
h_s	Sunrise time	h
Nu	Dimensionless Nusselt number	-

I_0	Solar illumination at the atmosphere top	$W.h.m^{-2}$
K	Wall conduction coefficient	$W.m^{-1}.K^{-1}$
P	Heat transfer fluid pressure	Pas
Q_{abs}	Amount of heat absorbed	$W.m^{-2}$
$Q_{émis}$	Amount of heat emitted	$W.m^{-2}$
φ	Latitude of the location	$(°)$
φ_i	Amount of elementary heat	W
ϕ_i	Amount of elementary heat emited	W
R	Thermal resistance of the wall	$m^2.K.W^{-1}$
t	Time	s
t_G	Overall calculation time	s
T	Temperature	$°C$
u	Fluid velocity along the (Ox) axis	$m.s^{-1}$
v	Fluid velocity along the (Oy) axis	$m.s^{-1}$
ZM	Sun azimuth	$(°)$
Greek letters		
α_i	Absorption coefficient of the material	-
δ	Phase shift time between maximum temperature and maximum radiation	h
λ	Thermal conductivity of the fluid	$W.m^{-1}.K^{-1}$
θ_{PS}	Inclination angle of the south wall	$(°)$
θ_{PN}	Inclination angle of the north wall	$(°)$
θ_{PO}	Inclination angle of the nest wall	$(°)$
θ_{PE}	Inclination angle of the east wall	$(°)$
θ_{PFP}	Inclination angle of the wall bottom ceiling	$(°)$
ρ	Density of the fluid	$Kg.m^{-3}$
Λ	Sunshine duration	h
ω	Hourly sun angle	$(°)$
ω_S	Hourly sunrise angle for a horizontal plane	$(°)$
Abbreviations		
GSF	Global solar flux	$W.m^{-2}$
GHSF	Global horizontal solar flux	$W.m^{-2}$
ISFS	Incident solar flux on the South wall	$W.m^{-2}$
ISFW	Incident solar flux on the West wall	$W.m^{-2}$
ISFE	Incident solar flux on the East wall	$W.m^{-2}$
HDIFR	Horizontal diffuse radiation	$W.m^{-2}$
HDIRR	Horizontal direct radiation	$W.m^{-2}$
GRIN	Global radiation incident on the North wall	$W.m^{-2}$
GRIS	Global radiation incident on the South wall	$W.m^{-2}$
GRIW	Global radiation incident on the West wall	$W.m^{-2}$
GRIE	Global radiation incident on the East wall	$W.m^{-2}$
URER'MS	Research Unit of Renewable Energies in Saharan Medium	-
T_{amb}	Ambient temperature	$(°C)$

References

[1] Yaïche, M. R. & Bekkouche, S.M.A. (2008). Conception et validation d'un programme sous Excel pour l'estimation du rayonnement solaire incident en Algérie. Cas d'un ciel totalement clair. *Revue des Énergies Renouvelables, 11*(3), 423–436.

[2] Yettou, F., Malek, A., Haddadi, M., & Gama, A. (2009). Étude comparative de deux modèles de calcul du rayonnement solaire par ciel clair en Algérie. *Revue des Énergies Renouvelables 12*(2), 331–346.

[3] Zarai, N., Chaabane, M., & Gabsi, S. (2010, November 5-7). *Outil de planification de la production thermique des capteurs solaires.* International Renewable Energy Congress*,* Sousse*,* Tunisia*.*

[4] Raad, A. (2017). *Co-simulation et optimisation multicritères en conception de bâtiment, par approche d'interopérabilité de services.* Grenoble Alpes Métropole, France: Université Grenoble Alpes

[5] Dinh, V. B., Delinchant, B., & Wurtz, F. (2016, June 7-9). *Dimensionnement optimal des systèmes énergétiques intégrant la stratégie de gestion pour une maison raccordée au réseau*. Symposium de Genie Electrique, Grenoble, France.

[6] Oudrane, A., Aour, B., Hamouda, M. & Benhamou, M. (2016). Méthodologie pour la détermination de l'écartement optimal de la chaîne tubulaire d'une dalle chauffante. *Revue des Énergies Renouvelables, 19*(1), 11–19.

[7] Hassine, N. B., Chesneau, X., & Laatar, A. H. (2017). Numerical simulation of heat and mass transfers during solar drying of sewage sludge: solar radiation effect*. Energy Procedia, 139*, 804–809.

[8] Oudrane, A., & Aour, B. (2017). Numerical investigation of a laminar flow in a tubular chain of a heated floor slab. *Recueil de mécanique, 2*(2), 192–203.

[9] Oudrane, A., Aour, B. & Hamouda, M. (2017). Numerical investigation of thermal exchanges for a habitable enclosure in a desert region. *International Journal of Renewable Energy, 12*(2), 87-105.

[10] Heuzé, T., Leblond, J. B., & Bergheau, J. M. (2011). Modélisation des couplages fluide/solide dans les procédés d'assemblage à haute température. *Mécanique et Industries, 12,* 183–191.

[11] Mladin, E., Lachi, M., & Padet, J. (2001). *Transfert de chaleur couplé conduction-convection en régime instationnaire, induit par une température imposée sur une plaque d'épaisseur finie.* Congrès Français de thermique, SFT2001, Nantes. pp.29-31.

[12] Pellegrin, N. D. (2016). *Modélisation fine des échanges thermiques entre les bâtiments et l'atmosphère urbaine*. Marne, France: Université Paris-Est Créteil Val.

[13] Mokhtari, F., Ait Messaoudéne, N., Hamid A., & Belhamel, M. (2006). Etude du comportement thermique d'une maison munie d'un système de chauffage solaire. *Revue des Energies Renouvelables, 9*(4), 363–370.

[14] Lantri, F., Bachari, N.I., & Belbachir, H. (2017). Estimation et cartographie des différentes composantes de rayonnement solaire au sol à partir des données météorologiques. *Revue des Energies Renouvelables. 20*(1), 111-130.

[15] Fiche Technique (Date de mise à jour : 22/06/2016) Tube PER Prégainé, 91, Rue Duruisseau, PA des Chesnes – 38297 St Quentin – Fallavier.

[16] Oudrane, A., Aour, B., & Benhamou, M. (2016). Étude et analyse paramétrique d'une installation solaire: plancher solaire dicte d'implanter dans la région d'Adrar. *El-Wahat pour les Recherches et les Études, 9*(1). 27 – 49.

[17] Moujalled, B. (2007). *Modélisation dynamique du confort thermique dans les bâtiments naturellement ventilés.* Villeurbanne, France: The Institut National des Sciences Appliquées de Lyon.

[18] Réglementations (201). ''Thermique acoustique aération des bâtiments d'habitation neufs dans les DOM, Fiche d'application – Thermique - Protection contre les rayonnements solaires''. Ministère de l'écologie du développement durable et de l'énergie.

[19] Inard, C., Depecker, P., & Roux, J. -J. (1997). Un modèle simplifié pour la prédiction du champ de température dans les bâtiments. *Rev. Gén. Therm, 36,* 113-l 23.

[20] Bouctouche, K. (2017). *Modélisation multi spectrale des images satellitaire - Application : quantification du bilan d'énergie sol-atmosphère*. Oran, Algérie : Laboratoire d'Analyse et d'Application des Rayonnements (LAAR).